



Universiteit
Leiden
The Netherlands

Intervention studies in a rat model of bronchopulmonary dysplasia : effects on cardiopulmonary injury and lung development

Visser, Y.P. de

Citation

Visser, Y. P. de. (2011, June 14). *Intervention studies in a rat model of bronchopulmonary dysplasia : effects on cardiopulmonary injury and lung development*. Retrieved from <https://hdl.handle.net/1887/17705>

Version: Corrected Publisher's Version

License: [Licence agreement concerning inclusion of doctoral thesis in the Institutional Repository of the University of Leiden](#)

Downloaded from: <https://hdl.handle.net/1887/17705>

Note: To cite this publication please use the final published version (if applicable).

Chapter 3

Phosphodiesterase-4-inhibition attenuates heart and lung injury by perinatal hyperoxia in neonatal and adult rats.

Submitted to Am J Physiol Lung Cell Mol Physiol 2011.

Abstract

Background: Phosphodiesterase (PDE) type 4 inhibitors are potent anti-inflammatory drugs with antihypertensive properties and their therapeutic role in bronchopulmonary dysplasia (BPD) is still controversial. We studied the role of PDE4 inhibition on normal lung development and its therapeutic value on pulmonary hypertension (PH) and right ventricular hypertrophy (RVH) in neonatal rats with hyperoxia-induced lung injury, a valuable model for premature infants with BPD. **Methods:** The cardiopulmonary effects of PDE4 inhibition with piclamilast treatment (5 mg/kg/day) were investigated in 2 models of experimental BPD: [1] daily treatment during continuous exposure to hyperoxia for 10 days and [2] a late treatment and injury-recovery model in which pups were exposed to hyperoxia or room air for 9 days, followed by 9 or 42 days of recovery in room air combined with treatment started on day 6 of oxygen exposure until day 18. **Results:** Prophylactic piclamilast treatment reduced pulmonary fibrin deposition, septum thickness, arteriolar wall thickness and RVH, and prolonged survival. In the late treatment and injury-recovery model hyperoxia caused persistent aberrant alveolar and vascular development, PH and RVH. Treatment with piclamilast in both models reduced arteriolar wall thickness, attenuated RVH and improved right ventricular function in the injury recovery model, but did not restore alveolarization or angiogenesis. Treatment with piclamilast did not show adverse cardiopulmonary effects in room air controls in both models. **Conclusions:** PDE4 inhibition attenuated and partially reversed PH and RVH, but did not advance alveolar development in neonatal rats exposed to hyperoxic lung injury or affect normal lung and heart development.

Introduction

The preterm lung is highly susceptible to injury during resuscitation, mechanical ventilation and pro-inflammatory mediators that may interfere with signalling pathways required for normal lung development and this may progress towards bronchopulmonary dysplasia (BPD), a chronic lung disease ¹. The hallmark in BPD is alveolar enlargement caused by an arrest in alveolar and vascular development. Serious complicating factors in the perinatal period are inflammation and oxidative stress and at later stages pulmonary hypertension (PH) due to elevated pulmonary artery pressure and pulmonary vascular resistance that increases afterload of the right ventricle and ultimately lead to right ventricular hypertrophy (RVH) and associated cardiac disease ¹⁻³. PH is characterized by persistent vasoconstriction and structural remodelling of the pulmonary blood vessels, including increased proliferation of vascular smooth muscle cells, which ultimately lead to high mortality in the absence of appropriate treatment due to right heart failure in children and adults ⁴⁻⁸.

Agents that elevate intracellular cGMP or cAMP levels exert therapeutic effects in experimental models of PH ⁹⁻¹². Phosphodiesterases (PDEs) inactivate the second messengers of important pulmonary vasodilator agents, including prostacyclin and nitric oxide, by hydrolysis. cAMP and its downstream target protein kinase A inhibit the extracellular signal-regulated kinase (ERK) activation and suppress the proliferation of pulmonary fibroblasts, vascular smooth muscle cells, airway epithelial cells and inflammatory cells ¹³. Among the eleven families of PDEs, the major cAMP-metabolizing enzymes are attributed to the PDE4 family ¹³⁻¹⁶, which consists of four genes (A-D) that are expressed in all immunocompetent cells, pulmonary artery smooth muscle cells ¹⁷, fibroblasts, endothelial and epithelial cells ¹³. We recently demonstrated in a hyperoxia-induced neonatal lung injury rat model that PDE4 inhibition improved survival and reduced lung injury by attenuating pulmonary inflammation ¹⁸.

The effect of PDE4 inhibition on cardiac disease in experimental BPD has to be elucidated, whereas the role of PDE4 inhibition on alveolarization in neonatal hyperoxic lung injury and in normal lung development in rodents is controversial ¹⁸⁻²⁰. Therefore, we studied the cardiopulmonary effects of the second generation PDE4 inhibitor piclamilast in neonatal rats with hyperoxia-induced BPD, using two different treatment strategies: 1) a prophylactic treatment strategy (early concurrent treatment) and 2) a more clinically relevant strategy, in which treatment was started after injury was induced (late treatment and injury-recovery). We demonstrated that prophylactic PDE4 inhibition with piclamilast in hyperoxia-induced neonatal lung injury improved angiogenesis and attenuated PH and RVH, but did not induce septation in the enlarged alveoli. In the injury-recovery model neonatal exposure to hyperoxia for 9 days induced persistent alveolar simplification, PH and RVH in young adult rats. Late treatment with piclamilast reversed established PH and RVH, but did not advance alveolar and pulmonary vascular development. Piclamilast treatment did not exert adverse effects on normal lung and heart development in both models, despite postnatal growth retardation.

Materials and Methods

Full methodological details are available in Appendice A.

Animals

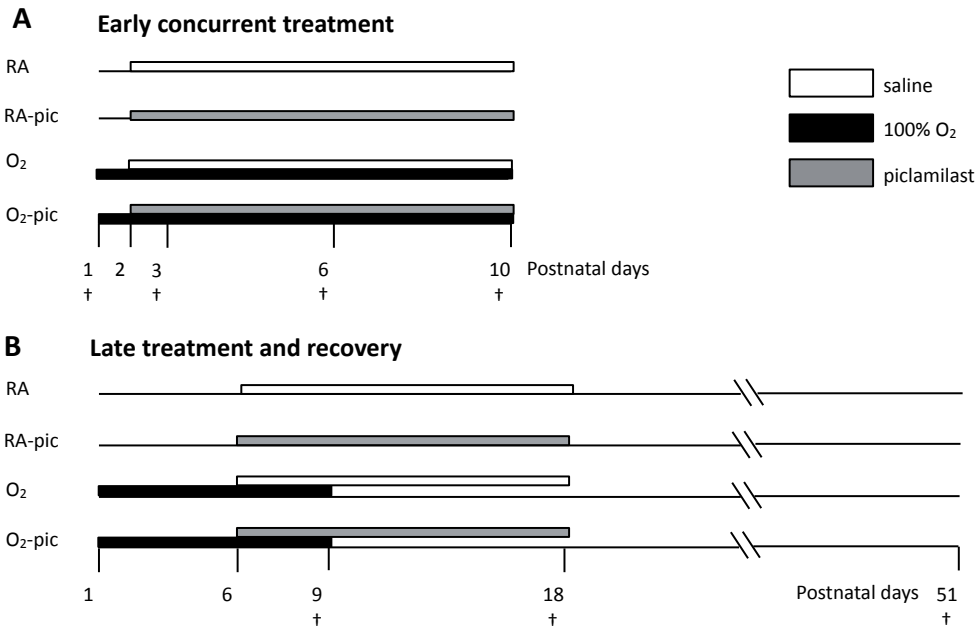
The research protocol was approved by the Institutional Animal Care and Use Committee of the Leiden University Medical Center. Neonatal rat pups were pooled and distributed over two experimental groups (N=12): an oxygen and oxygen-piclamilast group and two room air-exposed control groups injected either with saline or piclamilast. The oxygen concentration, body weight, evidence of disease and mortality were monitored daily.

Early concurrent treatment

Pups were continuously exposed to 100% oxygen for 10 days (Figure 1A). From day 2, pups received either 100 μ L piclamilast (5.0 mg/kg/day; a gift from Nycomed GmbH, Konstanz, Germany) in 0.9% saline (containing 0.05-0.1% DMSO) or daily 0.9% saline (containing 0.05-0.1% DMSO; 100 μ L), subcutaneously. Except for the survival experiments lung and heart tissue were collected on days 1, 3, 6 and 10. Separate experiments were performed for collection of lung and heart tissue for pulmonary fibrin deposition and RT-PCR (N=12), and histology (N=12).

Late treatment and recovery

Lung injury and recovery were investigated by exposing pups to hyperoxia for 9 days, followed by recovery in room air for 9 or 42 days (Figure 1B). After 6 days of hyperoxia daily injections with 100 μ L piclamilast (5.0 mg/kg/day) in 0.9% saline (containing 0.05-0.1% DMSO) or 100 μ L 0.9% saline (containing 0.05-0.1% DMSO) were started and continued throughout a 9-day recovery period in room air. Lung and heart tissues were collected for histology at the end of the 9-day hyperoxia period (N=8), after a 9-day recovery period in room air (N=8) and after 6-weeks of recovery in room air (N=8).

**Figure 1**

In the early concurrent treatment model for experimental BPD (panel A) neonatal rat pups were exposed to 100% oxygen (O₂; black bar) or room air (RA) directly after birth (day 1) until day 10. Treatment of RA and O₂ pups with piclamilast (10 mg/kg/day; gray bar) or 0.01% DMSO in 0.9% NaCl (white bar) was started on day 2 until day 10. Lung and heart tissues were harvested on days 1, 3, 6, and 10. In the late treatment and recovery model for experimental BPD (panel B) neonatal rat pups were exposed to O₂ (black bar) or RA directly after birth (day 1) until day 9. Hereafter pups were allowed to recover in RA up to day 51. Treatment with piclamilast (gray bar) or DMSO in 0.9% NaCl (white bar) was started on day 6 until day 18. Lung and heart tissues were harvested on days 9 (end hyperoxic period), 18 (end treatment period) and 51. Right ventricular function was determined on day 18.

Tissue preparation

Lungs and heart were snap-frozen in liquid nitrogen for real-time RT-PCR or fibrin deposition assay, and fixed in formalin for histology studies as previously described ^{11;12}.

Histology

Formalin-fixed, paraffin-embedded, 4 μm-thick heart and lung sections were stained with hematoxylin and eosin. Lungs were immunostained additionally with anti-ASMA (1:10,000), anti-vWF (1:4,000) or tenascin-C (1:500) using standard methods ^{11;12}. Quantitative morphometry was performed by two independent researchers blinded to the treatment strategy as previously described ^{12;21}.

Fibrin detection assay

Quantitative fibrin deposition in lung tissue homogenates was determined by Western blotting as described previously ^{11;22}.

Real-time RT-PCR

Total RNA isolation from lung and heart tissue homogenates, first-strand cDNA synthesis and real-time quantitative PCR were performed as described previously ^{12;22}. Primers are listed in Table 1.

Table 1. Sequences of Oligonucleotides used as Forward and Reverse Primers for Real-Time RT-PCR.

Gene Product	Primers	
	Forward Primer	Reverse Primer
ANP	5'-CCAGGCCATATTGGAGCAA-3'	5'-AGGTTCTTGAATCCATCAGATCTG-3'
BNP	5'-GAAGCTGCTGGAGCTGATAAGAG-3'	5'-TGTAGGGCCTGGTCCTTTG-3'
IL-6	5'-ATATGTTCTCAGGGAGATCTTGAA-3'	5'-TGCATCATCGCTGTTACATAAA-3'
TF	5'-CCCAGAAAGCATACCAAGTG-3'	5'-TGCTCCACAATGATGAGTGT-3'
VEGFA	5'-GCGGATCAAACCTCACAAA-3'	5'-TTGGTCTGCATTACATCTGCTA-3'
VEGFR2	5'-CCACCCAGAAATGTACCAAAC-3'	5'-AAAACGCGGTCTCTGGTT-3'
β-actin	5'-TTCAACACCCAGCCATGT-3'	5'-AGTGGTACGACCAGGCATACA-3'

Hemodynamic measurements

On day 18 RV pressure-volume loops were determined as previously described ²³. After anesthetized rats were mechanically ventilated, a combined pressure-conductance catheter (model FT212, SciSense, London, Ontario, Canada) was introduced via the apex into the RV and positioned towards the pulmonary valve. The catheter was connected to a signal processor (FV898 Control Box, SciSense) and RV pressures and volumes were recorded digitally and analyzed. After hemodynamic measurements, the heart was removed, fixed in buffered formaldehyde and processed for histology.

Statistical analysis

Values are expressed as mean ± SEM. Differences between groups (> 3) were analyzed with analysis of variance (ANOVA), followed by Tukey's multiple comparison test. For comparison of survival curves, Kaplan-Meier analysis followed by a log rank test was performed. Differences in the number of RVs positive for TN-C were analyzed with contingency table analysis followed by a Fisher's exact test. GraphPad Prism 5 (GraphPad Software, Inc, La Jolla, CA, USA) was used for statistical analysis. Differences at p values < 0.05 were considered statistically significant.

Results

Effects of piclamilast on pulmonary fibrin deposition and gene expression profiles

Prophylactic treatment model

To confirm the anti-inflammatory and angiogenic effects of piclamilast in neonatal chronic lung disease, demonstrated previously 18, fibrin deposition, a sensitive marker for tissue damage in hyperoxia-induced lung injury, and mRNA expression of IL6, TF, VEGFR2 and VEGFa were studied (Figure E1, Appendice A). A 9-fold hyperoxia-induced increase in pulmonary fibrin deposition was attenuated by 80% after piclamilast treatment for 10 days. Ten days of oxygen exposure increased the mRNA expression of IL6 (128-fold) and TF (4.6-fold) and decreased the expression of VEGFR2 (2.7-fold) and VEGFA (2.2-fold), which was attenuated by piclamilast treatment for 10 days as described previously 18.

Effects of piclamilast on growth and survival

Prophylactic treatment model

At birth, on postnatal day 1, mean body weight of the preterm rat pups was 5.2 g (Figure 2A). In room air-exposed control pups treated with 5.0 mg/kg/day of piclamilast growth was significantly retarded from day 5 onward compared to room air- and oxygen-exposed controls ($p < 0.05$; Figure 2A). Mean body weight of room air-exposed controls was 21.2 g and of oxygen-exposed pups 15.2 g on day 10. Piclamilast treatment significantly reduced body weight in room air- and oxygen-exposed pups to 13.2 and 10.6 g, respectively (Figure 2B). After 10 days of oxygen exposure, 77% of the oxygen-exposed control pups survived versus 100% of the pups of the other experimental groups ($p < 0.001$; Figure 2C).

Late treatment and injury-recovery model

On day 9, mean body weight of room-air pups was 17.8 ± 0.4 g (Figure 2D). On day 18, mean body weight was 32 ± 0.8 g and increased to 190 ± 7 g into adulthood on day 51. Mean body weight after 9 days of hyperoxia exposure was 13.3 ± 0.5 g. A recovery period of 42 days (day 51) in room air resulted in a significant difference between room air-exposed and oxygen-exposed controls (190 ± 7 g versus 165 ± 8 g, $p < 0.01$). Treatment of room air-controls and oxygen-exposed pups with piclamilast did not have a significant effect on mean body weight. On days 9, 18 and 51 all room air-exposed pups survived (Figure 2E). Exposure to hyperoxia for 9 days resulted in a 73% survival, which increased to 90% after treatment with piclamilast during the last 3 days of hyperoxia ($p < 0.001$). 80% of the pups that recovered in room air after hyperoxic lung injury survived until day 18 and >95% of the 18-day survivors were still alive on day 51. Survival on days 18 and 51 was not affected by piclamilast treatment.

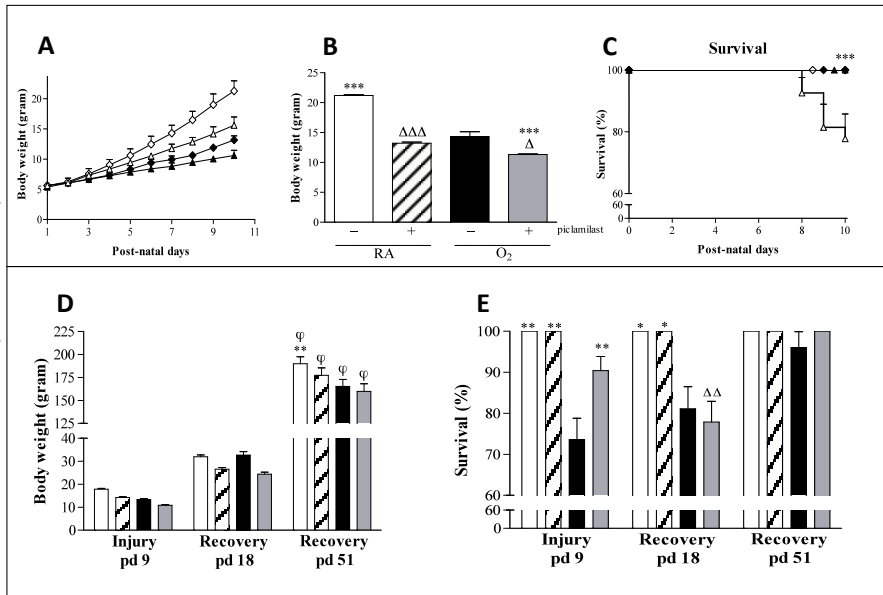


Figure 2

Growth (A), body weight (B and D) and survival (C and E) at day 10 after early concurrent treatment (N=12, A-C) and after late treatment and recovery (N=8, D and E) on days 9, 18 and 51 in room air controls (RA, white bars, \diamond), RA pups treated with 5.0 mg/kg/day piclamilast (striped bars, \blacklozenge), age-matched oxygen-exposed controls (black bars, Δ) and O₂ pups treated with 5.0 mg/kg/day piclamilast (gray bars, \blacktriangle). Growth and body weight are expressed as mean \pm SEM. Kaplan-Meier survival curve of piclamilast-treated O₂-exposed rat pups (\blacktriangle), age-matched O₂-exposed controls (Δ), RA-exposed controls (\diamond) and piclamilast-treated RA pups (\blacklozenge) during the first 10 days after birth (N=12, panel C). Survival data are expressed as percentage \pm SEM of pups surviving at the observed time point. $*p < 0.05$, $**p < 0.01$ and $***p < 0.001$ versus age-matched oxygen-exposed controls. $\Delta p < 0.05$, $\Delta\Delta p < 0.01$ and $\Delta\Delta\Delta p < 0.001$ versus room air-exposed pups treated with piclamilast. $\phi p < 0.001$ versus recovery on pd18.

Effects of piclamilast on lung airway development

Prophylactic treatment model

Lung development proceeds from the saccular stage at birth towards the alveolar stage on day 10 (Figure 3A). Treatment with piclamilast for 10 days during normal neonatal development did not result in differences in alveolar septum thickness, pulmonary vessel density, alveolar crest and arteriolar medial wall thickness compared to room air-exposed controls (Figure 3E-H). Oxygen exposure for 10 days resulted in lung edema, a heterogeneous distribution of enlarged air-spaces which were surrounded by septa with increased thickness (1.8-fold, $p < 0.001$; Figure 3C and F), a marked reduction in pulmonary vessel density (1.5-fold, $p < 0.001$ on day 6 and 3.8-fold, $p < 0.001$ on day 10; Figure 3E) and number of alveolar crests (3.7-fold, $p < 0.001$; Figure 3G), and an increase in arteriolar medial wall thickness (2.8-fold, $p < 0.001$; Figure 3H and K). Piclamilast treatment partially improved alveolar development during hyperoxia by thinning of alveolar septa (31%, $p < 0.01$; Figure 3D and F), increasing pulmonary vessel density (58.1%, $p < 0.05$ on day 10; Figure 3E) and reducing arteriolar

medial wall thickness (48.8%, $p < 0.001$; Figure 3H and L), but did not improve alveolar enlargement, determined by the number of alveolar crests per tissue ratio (Figure 3G) compared to oxygen exposure for 10 days.

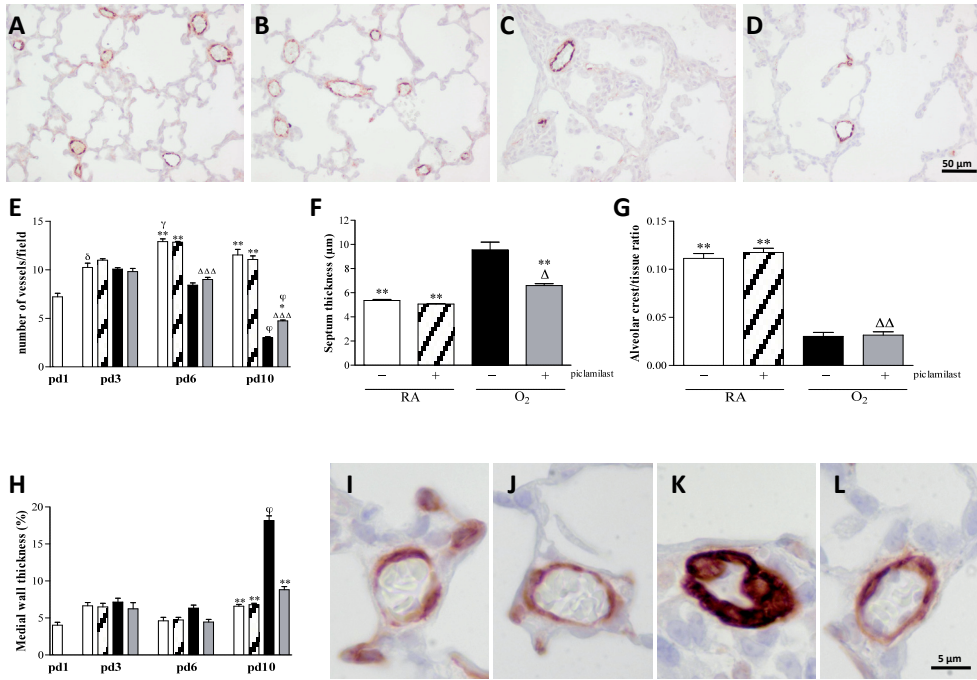


Figure 3

Lung sections stained for von Willebrand Factor (vWF; A-D) and for α smooth muscle actin (ASMA; I-L) and lung morphometry (E-H) of room air controls (RA, A and I, white bars), RA pups treated with 5.0 mg/kg/day piclamilast (B and J, striped bars), age-matched oxygen-exposed controls (O₂, C and K, black bars) and O₂ pups treated with 5.0 mg/kg/day piclamilast (D and L, gray bars) on day 10 (A-D, F, G and I-L) or on days 1, 3, 6 and 10 (E and H) after early concurrent treatment. Pictures were taken at a 200x magnification (vWF) and 1000x magnification (ASMA). Lung morphometry, including the quantifications of number of pulmonary vessels (E), septum thickness (F), alveolar crest per tissue ratio (G) and medial wall thickness (H) was determined on paraffin sections in RA and O₂ pups daily injected either with saline or piclamilast. Data are expressed as mean \pm SEM (N=12). * $p < 0.05$, and ** $p < 0.001$ versus age-matched oxygen-exposed controls. $\Delta p < 0.05$ and $\Delta\Delta p < 0.01$ versus room air-exposed pups treated with piclamilast. $\phi p < 0.001$ versus pd6. $\gamma p < 0.01$ versus pd3. $\delta p < 0.001$ versus pd 1.

Late treatment and injury-recovery model

Treatment of room air-exposed pups with piclamilast had no adverse effects on vascular (Figure 4A) and alveolar development (Figure 4B) and medial wall thickness (Figure 4C) on days 9, 18 and 51. Continuous neonatal exposure to hyperoxia for 9 days resulted in enlarged alveoli demonstrated by a 2.7-fold decrease in the number of alveolar crests ($p < 0.001$;

Figure 4B), and disturbed vascular development, demonstrated by a 2.5-fold reduction in blood vessel density ($p < 0.001$; Figure 4A) and a 2.4-fold increase in medial wall thickness ($p < 0.001$; Figure 4C) compared to room air controls. Piclamilast treatment during the last 3 days of the injurious hyperoxic period from day 6 to day 9 did not improve alveolarization, vascular development and medial wall thickness. A recovery period of 9 days in room air after hyperoxia-induced lung injury had a minor beneficial effect on the number of alveolar crests ($p < 0.001$; Figure 4B) and blood vessel density ($p < 0.001$; Figure 4A), but no effect on medial wall thickness (Figure 4C). Treatment with piclamilast did not improve alveolarization and vascular development, but reduced significantly medial wall thickness by 42.7% ($p < 0.001$; Figure 4C) in comparison with non-treated hyperoxia-exposed pups at the end of the recovery period on day 18. A recovery period of 42 days in room air after hyperoxia-induced lung injury had only a minor beneficial effect on the number of blood vessels on day 51 ($p < 0.01$; Figure 4A), but no improvement on alveolarization or medial wall thickness. Treatment with piclamilast did not improve alveolarization and vascular development, but reduced medial wall thickness by 45.9% ($p < 0.001$; Figure 4C) in comparison with non-treated hyperoxia-exposed pups at the end of the recovery period on day 51.

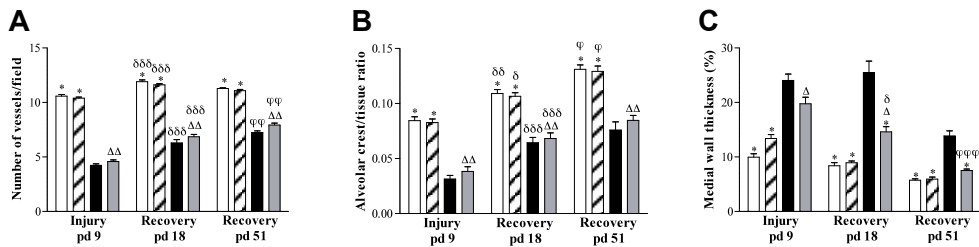


Figure 4

Quantification of number of pulmonary vessels (A), alveolar crest per tissue ratio (B) and medial wall thickness (C) determined on paraffin sections after late treatment and recovery on days 9, 18 and 51 in room air controls (RA, white bars), RA pups treated with 5.0 mg/kg/day piclamilast (striped bars), age-matched oxygen-exposed controls (O₂, black bars) and O₂ pups treated with 5.0 mg/kg/day piclamilast (gray bars). Data are expressed as mean \pm SEM (N=8). * $p < 0.001$ versus age-matched oxygen-exposed controls. $\Delta p < 0.01$ and $\Delta\Delta p < 0.001$ versus room air-exposed pups treated with piclamilast. $\delta p < 0.05$, $\delta\delta p < 0.01$ and $\delta\delta\delta p < 0.001$ versus recovery on pd9. $\phi p < 0.05$, $\phi\phi p < 0.01$ and $\phi\phi\phi p < 0.001$ versus recovery on pd18.

Heart development and right ventricular hypertrophy

Prophylactic treatment model

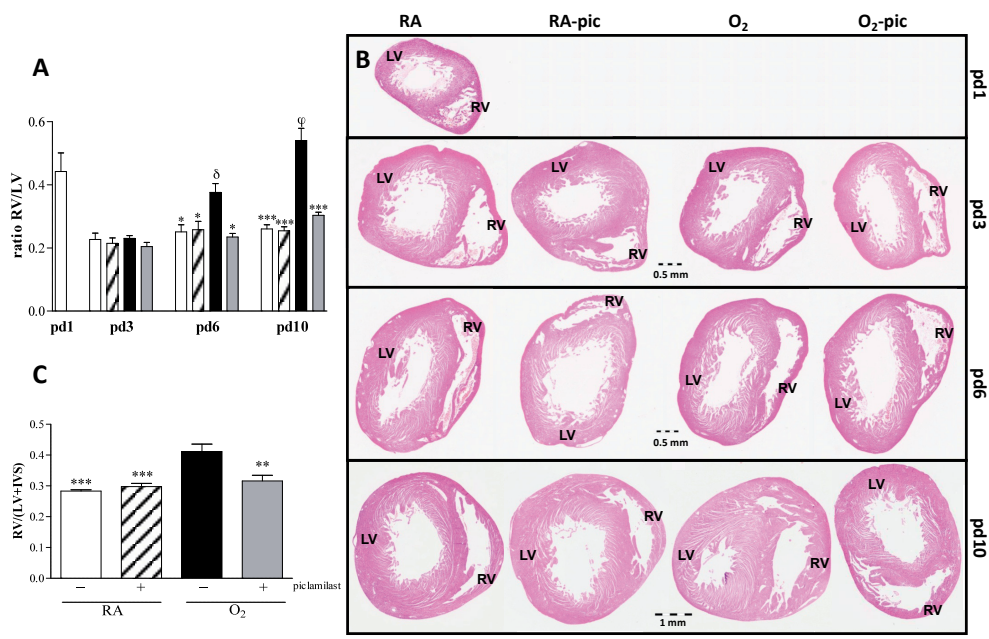
At birth the ratio between RV and LV free wall thickness was 0.44, decreased to 0.23 on day 3 and did not change hereafter until day 10 (Figure 5A). Treatment of control pups with piclamilast did not result in any differences in cardiac characteristics (Figure 5A-C, and Table 2). Exposure to hyperoxia resulted in a gradual development of RVH as demonstrated by an 1.5-fold ($p < 0.05$) and a 2.1-fold ($p < 0.001$) increase in the ratio between RV and LV free wall thickness and an 1.6-fold ($p < 0.05$) and a 2.2-fold ($p < 0.001$) increase in RV free wall

thickness on days 6 and 10, respectively, which was completely prevented by treatment with piclamilast (Figure 5A and B, and Table 2). Exposure to hyperoxia showed a tendency towards an increase in IVS thickness, but did not have a significant effect on LV free wall and IVS thickness (Figure 5B and Table 2). Because the hyperoxia-induced increase in RV free wall thickness was highest on day 10, we also studied the weight ratio RV/(LV + IVS) as an additional marker of RVH on day 10 (Figure 5C). Exposure to hyperoxia for 10 days resulted in an 1.5-fold increase in the RV/(LV + IVS) weight ratio ($p < 0.001$; Figure 5C), which was prevented by treatment with piclamilast.

Table 2. Cardiac Characteristics in early concurrent treatment

	day	RA		O ₂	
		saline	piclamilast	saline	piclamilast
RV free wall thickness $\mu\text{m}/\sqrt[3]{\text{BW}}$	1	85 ± 8	n.a.	n.a.	n.a.
	3	59 ± 3	54 ± 4	58 ± 3	47 ± 3
	6	71 ± 4*	65 ± 7**	112 ± 5 ^δ	63 ± 4**
	10	85 ± 7***	85 ± 4***	184 ± 13 ^φ	111 ± 4***, φφ
IVS thickness $\mu\text{m}/\sqrt[3]{\text{BW}}$	1	169 ± 10	n.a.	n.a.	n.a.
	3	216 ± 7	212 ± 12	191 ± 7	186 ± 7
	6	267 ± 11	213 ± 10**	309 ± 14 ^δ	250 ± 8
	10	289 ± 26	302 ± 10 ^φ	324 ± 13	264 ± 6*
LV free wall thickness $\mu\text{m}/\sqrt[3]{\text{BW}}$	1	200 ± 11	n.a.	n.a.	n.a.
	3	257 ± 12	256 ± 13	252 ± 5	231 ± 8
	6	289 ± 12	253 ± 9	303 ± 11	270 ± 14
	10	329 ± 26	336 ± 5 ^φ	343 ± 9	367 ± 7 ^{φφ}

n.a. = not applicable. * $p < 0.05$, ** $p < 0.01$ and *** $p < 0.001$ versus age-matched O₂ exposed controls. ^Δ $p < 0.05$ versus room air (RA) exposed controls. ^δ $p < 0.001$ versus pd3. ^φ $p < 0.01$ and ^{φφ} $p < 0.001$ versus pd6

**Figure 5**

Ventricular free wall thickness, indicated as the RV/LV ratio (A) and right ventricular hypertrophy depicted as the ratio RV/(LV+IVS) (C) in room air-exposed controls (RA, white bars), room air-exposed pups treated with piclamilast (5.0 mg/kg/day; striped bar), age-matched oxygen-exposed controls (O₂, black bar) and O₂ pups treated with piclamilast (5.0 mg/kg/day; gray bar) on day 10 (C) or on days 1, 3, 6 and 10 (A and B) after early concurrent treatment. Data are expressed as mean ± SEM (N=12). Paraffin heart sections stained with haematoxylin and eosin at a 100x magnification (B) in room-air controls (RA), RA pups treated with 5.0 mg/kg/day of piclamilast (RA-pic), oxygen controls (O₂) and O₂ pups treated with 5.0 mg/kg/day of piclamilast (O₂-pic) on days 1, 3, 6 and 10. IVS = interventricular septum, LV = left ventricle, RV = right ventricle. **p* < 0.05, ***p* < 0.01 and ****p* < 0.001 versus age-matched O₂-exposed controls. δ *p* < 0.01 versus pd3. ϕ *p* < 0.01, versus pd6.

Extracellular expression of tenascin-C, a marker of myocardial overload, was visible in the RV only after exposure to hyperoxia (Figure 6C, Table 3). Piclamilast treatment decreased the number of RVs positive for tenascin-C by 90% (*p* < 0.05, Figure 6D, Table 3). Extravascular tenascin-C expression was absent in room air-exposed controls either injected with saline or 5.0 mg/kg/day of piclamilast (Figure 6A and B, Table 3).

Table 3. Protein expression of Tenascin C in the right ventricular free wall

Treatment	saline positive TNC (n)	piclamilast positive TNC (n)
RA	0 (12)	0 (10)
O ₂	11 (12)	1 (12)*

**p* < 0.05 versus age-matched O₂ exposed controls

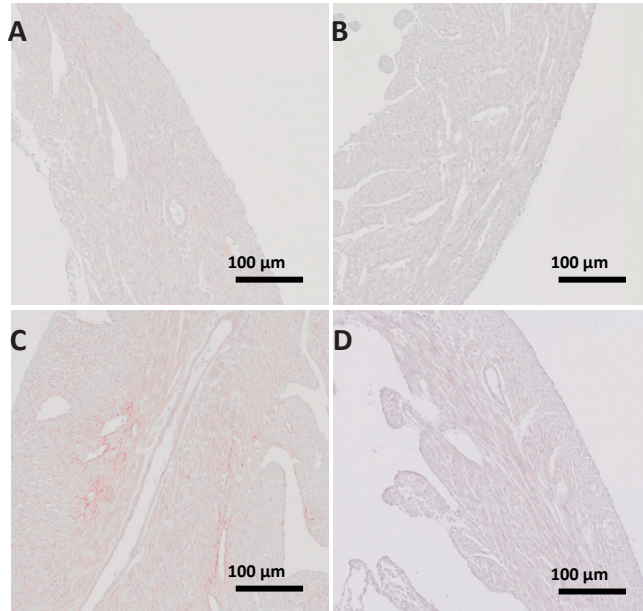


Figure 6

Paraffin sections of the right ventricular free wall stained with polyclonal tenascin C (A-D) of room-air controls (RA, A), RA pups treated with 5.0 mg/kg/day of piclamilast (RA-pic, B), oxygen controls (O₂, C) and O₂ pups treated with 5.0 mg/kg/day of piclamilast (O₂-pic, D) at 10 days after early concurrent treatment. Note the expression of tenascin C in the right ventricle in oxygen-exposed pups (C) and the absence of staining after treatment with piclamilast (B and D) and in room air controls (A). Pictures were taken at a 200x magnification.

Late treatment and injury-recovery model

Treatment of room air-exposed control pups with piclamilast had no effect on cardiac characteristics (Figure 7A and B, and Table 4). Nine days of hyperoxic lung injury resulted in an 1.3-fold increase in the ratio RV/LV wall thickness ($p < 0.01$; Figure 7A and B) and an 1.4-fold increase in RV free wall thickness compared to room air-controls ($p < 0.05$; Table 4). A recovery period of 9 (day 18) or 42 (day 51) days did not reduce hyperoxia-induced RVH in the non-treated pups, but treatment with piclamilast attenuated hyperoxia-induced RVH on days 9, 18 and 51 (Figure 7A and B, and Table 4).

Table 4. Cardiac Characteristics in late treatment and recovery

	day	RA		O ₂	
		saline	piclamilast	saline	piclamilast
RV free wall thickness $\mu\text{m}/\sqrt[3]{\text{BW}}$	9	100 ± 7*	107 ± 4	142 ± 10	118 ± 9
	18	96 ± 9***	110 ± 5***	179 ± 9	140 ± 10*
	51	96 ± 2***	98 ± 2***	160 ± 7	113 ± 4**
IVS thickness $\mu\text{m}/\sqrt[3]{\text{BW}}$	9	284 ± 7	288 ± 11	299 ± 15	288 ± 13
	18	265 ± 16	278 ± 8	283 ± 21	319 ± 16
	51	293 ± 6	292 ± 8	299 ± 8	286 ± 13
LV free wall thickness $\mu\text{m}/\sqrt[3]{\text{BW}}$	9	281 ± 7	289 ± 11	306 ± 11	334 ± 9
	18	277 ± 14*	292 ± 5	331 ± 19	366 ± 14 ^Δ
	51	342 ± 5 ^δ	329 ± 6	358 ± 12	368 ± 7

* $p < 0.05$, ** $p < 0.01$ and *** $p < 0.001$ versus age-matched O₂ exposed controls. ^Δ $p < 0.001$ versus room air (RA) exposed controls. ^δ $p < 0.001$ versus pd18.

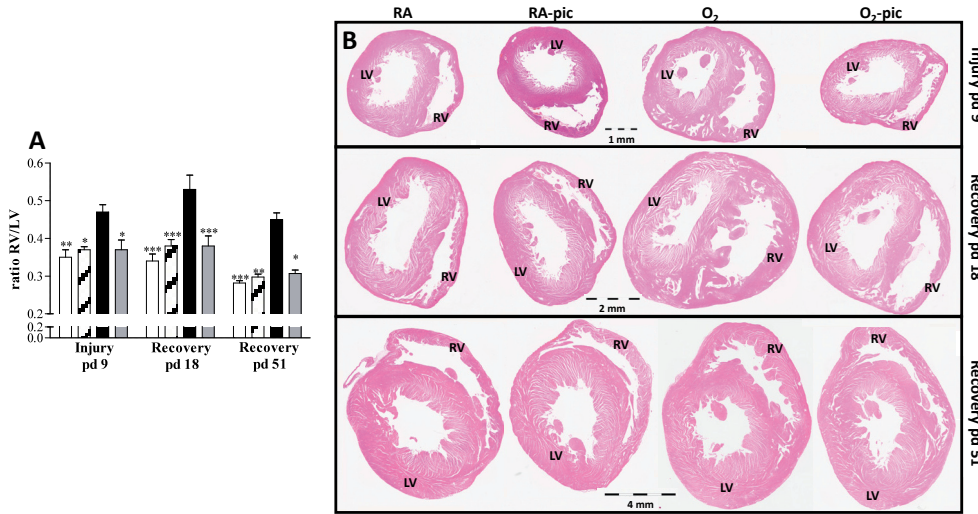


Figure 7

Right ventricular hypertrophy depicted as the RV/LV ratio (A), after late treatment and recovery on days 9, 18 and 51 in room air controls (RA, white bars), RA pups treated with 5.0 mg/kg/day of piclamilast (striped bars), age-matched oxygen-exposed controls (black bars) and O₂ pups treated with 5.0 mg/kg/day of piclamilast (gray bars). Paraffin heart sections stained with haematoxylin and eosin at a 100 times magnification (B) in room-air controls (RA), RA pups treated with 5.0 mg/kg/day of piclamilast (RA-pic), oxygen controls (O₂) and O₂ pups treated with 5.0 mg/kg/day of piclamilast (O₂-pic) on days 9, 18 and 51. Data are expressed as mean ± SEM (N=8). * $p < 0.05$, ** $p < 0.01$ and *** $p < 0.001$ versus age-matched O₂-exposed controls.

Cardiac mRNA expression

Prophylactic treatment model

Exposure to hyperoxia for 10 days increased RV mRNA expression for the natriuretic peptides ANP (13-fold; $p < 0.001$, Figure 8A) and BNP (17-fold; $p < 0.001$, Figure 8B) compared to room air-controls. Treatment with piclamilast during hyperoxia decreased the expression of ANP (by 54%; $p < 0.05$) and BNP (by 64%; $p < 0.001$) compared to oxygen-exposed controls. Exposure to hyperoxia for 10 days increased mRNA expression in the left ventricle plus interventricular septum (LV + IVS) for the natriuretic peptides ANP (3.7-fold; $p < 0.001$, Figure 8A) and BNP (3.1-fold; $p < 0.001$, Figure 8B) compared to room air-controls. In LV + IVS treatment with piclamilast decreased the expression of BNP (by 30%; $p < 0.05$) compared to oxygen-exposed controls.

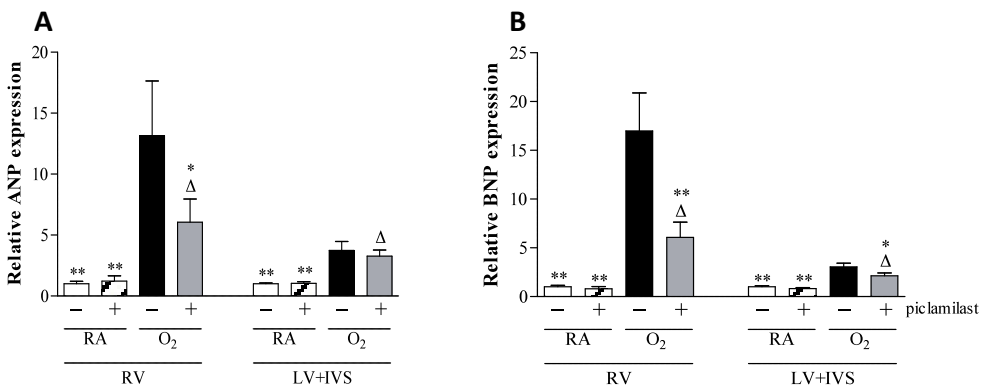


Figure 8

Relative mRNA expression in the right ventricular free wall (RV) and left ventricle, including the interventricular septum (LV + IVS), determined with RT-PCR, of atrial natriuretic peptide (ANP; A) and brain natriuretic peptide (BNP; B) in room air-exposed controls (RA, white bars), room air-exposed pups treated with piclamilast (5.0 mg/kg/day; striped bar), age-matched oxygen-exposed controls (O₂, black bar) and O₂ pups treated with piclamilast (5.0 mg/kg/day; gray bar) on day 10 after early concurrent treatment. Data are expressed as mean \pm SEM (N=12). * $p < 0.05$ and ** $p < 0.001$ versus age-matched oxygen-exposed controls. $\Delta p < 0.001$ versus room air-exposed controls treated with piclamilast.

Right ventricular function

Late treatment and injury-recovery model

Treatment of room air-exposed control pups with piclamilast slowed down relaxation ($p < 0.05$) on day 18 (Table 5). After a hyperoxic period of 9 days and 9 days of recovery peak RV pressure and end-systolic RV pressure were elevated ($p < 0.001$), compared to room air-controls, demonstrating hyperoxia-induced PH. Volumetric indices and cardiac output were maintained despite the increased afterload. Systolic function reflected by ejection fraction tended to be improved. Treatment with piclamilast reduced hyperoxia-induced peak RV

pressure and end-systolic pressure by 20% ($p < 0.05$) compared to oxygen-exposed controls, demonstrating that piclamilast attenuated hyperoxia-induced PH on day 18.

Table 5. Right ventricular function in late treatment and recovery at pd 18

Right ventricle	unit	RA		O ₂	
		saline	piclamilast	saline	piclamilast
<i>General hemodynamics</i>					
Stroke volume	μl/g	1.12 ± 0.10	1.18 ± 0.14	1.27 ± 0.13	1.07 ± 0.12
Cardiac index	(ml/g)/min	0.34 ± 0.03	0.28 ± 0.03	0.41 ± 0.05	0.26 ± 0.03*
Stroke work	mmHg.(μl/g)	15.5 ± 1.5***	19.2 ± 2.1**	42.4 ± 6.5	27.7 ± 3.4
<i>Systolic function</i>					
Peak RV pressure	mmHg	17.4 ± 0.8***	22.0 ± 1.5***	43.5 ± 3.7	34.9 ± 1.9*, ^{ΔΔ}
End-systolic pressure	mmHg	15.3 ± 0.9***	20.2 ± 1.4***	39.1 ± 3.3	32.1 ± 1.9*, ^{ΔΔ}
End-systolic volume	μl/g	1.18 ± 0.15	0.88 ± 0.13	1.06 ± 0.13	0.83 ± 0.27
Ejection fraction	%	49.2 ± 3.7	57.5 ± 4.6	54.3 ± 3.6	63.6 ± 7.0
<i>Diastolic function</i>					
End-diastolic pressure	mmHg	2.8 ± 0.5	3.3 ± 0.5	4.9 ± 0.4	4.9 ± 0.7 ^Δ
End-diastolic volume	μl/g	2.30 ± 0.18	2.06 ± 0.18	2.33 ± 0.22	1.90 ± 0.27
Relaxation time constant	ms	17.7 ± 1.5	23.3 ± 1.1***, ^Δ	15.6 ± 1.0	24.8 ± 1.4***

NB: All volumetric indices were indexed for body weight.* $p < 0.05$, ** $p < 0.01$ and *** $p < 0.001$ versus age-matched O₂ exposed controls. ^Δ $p < 0.05$ and ^{ΔΔ} $p < 0.01$ versus room air (RA) exposed controls.

Discussion

Our data demonstrate that prophylactic treatment with piclamilast, a specific second generation PDE4 inhibitor, prolongs survival and prevents cardiopulmonary disease in neonatal rat pups with hyperoxia-induced chronic lung disease, a valuable model for bronchopulmonary dysplasia in preterm infants²², by preventing the development of PH and RVH, and attenuating lung inflammation, alveolar septum thickness, impaired angiogenesis and vascular arteriolar remodelling. Early exposure to hyperoxia for 9 days in the neonatal period causes persistent alveolar simplification, PH and RVH in neonatal and adult rats. Piclamilast treatment reverses established PH and RVH in hyperoxia-exposed rat pups and in adult survivors of hyperoxic lung injury in an injury-recovery model, but does not reverse hyperoxia-induced alveolar enlargement in neonatal and adult rats.

Prophylactic piclamilast treatment improved hyperoxia-induced RVH, as shown by reduced thickness and weight of the RV, and reduced ANP, BNP and extracellular tenascin-C expression in the RV, markers that are upregulated under myocardial stress conditions^{24;25}. Although PDE4 is expressed in the mammalian heart the therapeutic effects of PDE4 inhibitors in cardiac disease are still unclear²⁶. The beneficial effect of piclamilast on the heart can be explained indirectly by a decrease in pulmonary arteriolar wall thickness resulting in less vasoconstriction and PH, and, as a result, reduced RVH. Vasoconstriction and remodelling of pulmonary blood vessels with proliferation of smooth muscle cells and fibroblasts in pulmonary vessels are important contributors to PH^{8;27}. The importance of smooth muscle

cells in the therapeutic effect of PDE3 and -4 inhibitors in PH is supported by [1] a reduced proliferation of pulmonary artery smooth muscle cells by cAMP²⁸, [2] a high activity of PDE3 and -4 in these cells²⁹ and [3] the beneficial effects of PDE3 and/or -4 inhibitors on vascular remodelling, vasoconstriction and RVH in experimental models *in vivo*, including hyperoxia-induced neonatal lung injury (this study), monocrotaline- or hypoxia-induced PH^{10;29}, bleomycin-induced pulmonary fibrosis³⁰ and *in vitro* studies with human pulmonary artery smooth muscle cells³¹. In addition, PDE4 inhibition reduces the expression of endothelin-1, a potent vasoconstrictor and stimulator of the proliferation of vascular smooth-muscle cells^{30;32}. Studies with prostacyclin analogs, which induce relaxation of vascular smooth muscle by stimulating the production of cAMP and subsequently inhibit the proliferation of SMCs, have shown a decrease in pulmonary arterial hypertension *in vitro* and *in vivo*^{33;34}. Since pro-inflammatory cytokines and chemokines can stimulate pulmonary artery smooth muscle cell proliferation³⁵, the therapeutic effect of PDE4 inhibition on PH in experimental BPD may be, at least partially, indirect via inhibition of the inflammatory response, which is an important contributor to experimental BPD as demonstrated previously in neonatal hyperoxia-induced lung disease^{18;19}.

Hyperoxia-induced RVH, which can be detected from neonatal day 6 onward, precedes the detection of PH, determined by arteriolar wall thickness, which can be detected from neonatal day 9 onwards. Since RVH is a direct consequence of PH these unexpected results may be explained by increased vasoconstriction rather than proliferation of vascular smooth muscle cells in small pulmonary arterioles and/or a reduction of the pulmonary vascular bed as demonstrated by a decrease in pulmonary vascular density from day 6 onward.

Recent data on PDE4 inhibition in hyperoxia-induced neonatal lung injury show conflicting effects on alveolarization in rodents. In neonatal rats with an ongoing lung injury due to oxidative stress and inflammation, piclamilast did not protect against impaired alveolarization [this study and^{18;19}], but in a less aggressive model of hyperoxic lung injury in neonatal mice, PDE4 inhibition with cilomilast enhanced lung alveolarization²⁰. These contradictory findings may be explained by differences in oxidative stress (100% versus 85% oxygen), duration of hyperoxia (10 days versus 28 days), start of treatment (starting on day 1 versus 14), the PDE4 inhibitor used (rolipram, piclamilast and cilomilast) and species (rats versus mice). In contrast with cilomilast treatment, rolipram and piclamilast treatment reduces body weight gain which will associate with decreases in lung volumes and absolute alveolar surface area³⁶. However, we did not find any effect of PDE4 inhibition on normal lung development, i.e. alveolarization and angiogenesis were normal, despite a reduction in body weight gain compared with untreated normal rats [this study and^{18;19}].

Hyperoxia leads to impaired alveolar and lung vascular development, which may be explained by disruption of VEGF signalling^{4;18;37;38}. In this study, PDE4 inhibition by piclamilast attenuated the hyperoxia-induced impairment of angiogenesis, but not the impaired alveolarization, by increasing VEGFa and VEGF receptor-2 (VEGFR2) mRNA expression in the lung. Initiation of angiogenesis involves migration and VEGF-induced proliferation of vascular endothelial cells. However, the VEGF-induced proliferation of vascular endothelial cells is associated with augmented cAMP hydrolysis by up-regulating PDE4 isozymes³⁹ and is inhibited by cAMP elevating drugs^{40;41}. Recombinant human VEGF treatment enhances alveolarization and vessel growth and improves lung structure in hyperoxia-induced lung injury in newborn rats^{42;43}, whereas VEGF blockade impairs alveolarization and vessel

growth³⁸. We assume that the piclamilast-induced increase in pulmonary VEGFa and VEGFR2 mRNA levels was not sufficient to advance alveolarization.

Although treatment of oxygen-exposed rat pups with piclamilast resulted, as expected, in a decrease in end-systolic and peak systolic RV pressure, this effect of PDE4 inhibition on heart pressure was less than expected from our morphometric data on lung arteriolar wall thickness and RVH (RV free wall thickness, relative to the LV). This discrepancy can be explained by (1) a reduction of the pulmonary vascular bed, as demonstrated by a persistent decrease in hyperoxia-induced vascular density that can not be restored after piclamilast treatment, and/or (2) a direct effect of PDE4 inhibition on the myocardium resulting in enhanced contractility of the RV due to increased intracellular cAMP levels in cardiomyocytes. Elevated cAMP levels after β -adrenergic-dependent signalling are associated with a positive inotropic effect, resulting in protein kinase A (PKA)-dependent phosphorylation of multiple proteins involved in the regulation of the cytosolic Ca²⁺ concentration, including the sarcoplasmic reticulum Ca²⁺ release channel (ryanodine receptor), the sarcoplasmic reticulum Ca²⁺ ATPase (SERCA), and its regulatory protein phospholamban and the Na⁺-Ca²⁺ exchanger regulatory protein phospholemman²⁶. Piclamilast-induced enhanced contractility of the RV can explain, at least in part, the limited increase in RV free wall thickness in piclamilast treated oxygen-exposed rats despite an elevated RV peak pressure.

Perspectives

If we can extrapolate these findings in hyperoxia-exposed neonatal rats to preterm infants with respiratory failure, we might expect a beneficial effect of piclamilast on both PH and RVH, which are often the major reason for mortality or severe morbidity in preterm infants. A recent systematic review has shown that the clinical use of inhaled nitric oxide in preterm infants with respiratory failure does not significantly reduce neonatal mortality or bronchopulmonary dysplasia⁴⁴. Our data warrant clinical investigation of piclamilast as a potential drug to prevent or treat PH and RVH which play a pivotal role in poor outcome in the neonatal nursery.

References

1. Baraldi E, Filippone M. Chronic lung disease after premature birth. *N Engl J Med* 2007;357:1946-1955.
2. Jobe AH, Bancalari E. Bronchopulmonary dysplasia. *Am J Respir Crit Care Med* 2001;163:1723-1729.
3. Kinsella JP, Greenough A, Abman SH. Bronchopulmonary dysplasia. *Lancet* 2006;367:1421-1431.
4. Abman SH. Recent advances in the pathogenesis and treatment of persistent pulmonary hypertension of the newborn. *Neonatology* 2007;91:283-290.
5. Tuder RM, Abman SH, Braun T, Capron F, Stevens T, Thistlethwaite PA, Haworth SG. Development and pathology of pulmonary hypertension. *J Am Coll Cardiol* 2009;54:S3-S9.
6. Steinhorn RH. Neonatal pulmonary hypertension. *Pediatr Crit Care Med* 2010;11:S79-S84.
7. Abman SH. Pulmonary hypertension in children: a historical overview. *Pediatr Crit Care Med* 2010;11:S4-S9.
8. Humbert M, Sitbon O, Simonneau G. Treatment of pulmonary arterial hypertension. *N Engl J Med* 2004;351:1425-1436.
9. Schermuly RT, Kreisselmeier KP, Ghofrani HA, Yilmaz H, Butrous G, Ermert L, Ermert M, Weissmann N, Rose F, Guenther A. Chronic sildenafil treatment inhibits monocrotaline-induced pulmonary hypertension in rats. *Am J Respir Crit Care Med* 2004;169:39-45.
10. Izikki M, Raffestin B, Klar J, Hatzelmann A, Marx D, Tenor H, Zadigue P, Adnot S, Eddahibi S. Effects of roflumilast, a phosphodiesterase-4 inhibitor, on hypoxia- and monocrotaline-induced pulmonary hypertension in rats. *J Pharmacol Exp Ther* 2009;330:54-62.

11. de Visser YP, Walther FJ, Laghmani EH, van der Laarse A, Wagenaar. GT Apelin attenuates hyperoxic lung and heart injury in neonatal rats. *Am J Respir Crit Care Med* 2010;182:1239-1250.
12. de Visser YP, Walther FJ, Laghmani EH, Boersma H, van der Laarse A, Wagenaar GT. Sildenafil attenuates pulmonary inflammation and fibrin deposition, mortality and right ventricular hypertrophy in neonatal hyperoxic lung injury. *Respir Res* 2009;10:30-42.
13. Torphy TJ. Phosphodiesterase isozymes: molecular targets for novel antiasthma agents. *Am J Respir Crit Care Med* 1998;157:351-370.
14. Conti M, Richter W, Mehats C, Livera G, Park JY, Jin C. Cyclic AMP-specific PDE4 phosphodiesterases as critical components of cyclic AMP signaling. *J Biol Chem* 2003;278:5493-5496.
15. Essayan DM. Cyclic nucleotide phosphodiesterases. *J Allergy Clin Immunol* 2001;108:671-680.
16. Fan CK. Phosphodiesterase inhibitors in airways disease. *Eur J Pharmacol* 2006;533:110-117.
17. Millen J, MacLean MR, Houslay MD. Hypoxia-induced remodelling of PDE4 isoform expression and cAMP handling in human pulmonary artery smooth muscle cells. *Eur J Cell Biol* 2006;85:679-691.
18. de Visser YP, Walther FJ, Laghmani EH, van Wijngaarden S, Nieuwland K, Wagenaar GT. Phosphodiesterase-4 inhibition attenuates pulmonary inflammation in neonatal lung injury. *Eur Respir J* 2008;31:633-644.
19. Mehats C, Franco-Montoya ML, Boucherat O, Lopez E, Schmitz T, Zana E, Evain-Brion D, Bourbon J, Delacourt C, Jarreau PH. Effects of phosphodiesterase 4 inhibition on alveolarization and hyperoxia toxicity in newborn rats. *PLoS One* 2008;3:e3445.
20. Woyda K, Koebrich S, Reiss I, Rudloff S, Pullamsetti SS, Ruhlmann A, Weissmann N, Ghofrani HA, Gunther A, Seeger W. Inhibition of phosphodiesterase 4 enhances lung alveolarisation in neonatal mice exposed to hyperoxia. *Eur Respir J* 2009;33:861-870.
21. Yi M, Jankov RP, Belcastro R, Humes D, Copland I, Shek S, Sweezey NB, Post M, K. Albertine H, Auten RL. Opposing effects of 60% oxygen and neutrophil influx on alveologenesis in the neonatal rat. *Am J Respir Crit Care Med* 2004;170:1188-1196.
22. Wagenaar GT, ter Horst SA, van Gastelen MA, Leijser LM, Mauad T, van der Velden PA, de Heer E, Hiemstra PS, Poorthuis BJ, Walther FJ. Gene expression profile and histopathology of experimental bronchopulmonary dysplasia induced by prolonged oxidative stress. *Free Radic Biol Med* 2004;36:782-801.
23. Hessel MH, Steendijk P, den Adel B, Schutte CI, van der Laarse A. Characterization of right ventricular function after monocrotaline-induced pulmonary hypertension in the intact rat. *Am J Physiol Heart Circ Physiol* 2006;291:H2424-H2430.
24. Boerma M, van der Wees CG, Vrieling H, Svensson JP, Wondergem J, van der, Laarse LA. Mullenders H, van Zeeland AA. Microarray analysis of gene expression profiles of cardiac myocytes and fibroblasts after mechanical stress, ionising or ultraviolet radiation. *BMC Genomics* 2005;6:6.
25. Yamamoto K, Dang QN, Kennedy SP, Osathanondh R, Kelly RA, Lee RT. Induction of tenascin-C in cardiac myocytes by mechanical deformation. Role of reactive oxygen species. *J Biol Chem* 1999;274:21840-21846.
26. Rao YJ, Xi L. Pivotal effects of phosphodiesterase inhibitors on myocyte contractility and viability in normal and ischemic hearts. *Acta Pharmacol Sin.* 2009;30:1-24.
27. Abman SH. Impaired vascular endothelial growth factor signaling in the pathogenesis of neonatal pulmonary vascular disease. *Adv Exp Med Biol* 2010;661:323-335.
28. Rybalkin SD, Bornfeldt KE. Cyclic nucleotide phosphodiesterases and human arterial smooth muscle cell proliferation. *Thromb Haemost.* 1999;82:424-434.
29. Phillips PG, Long L, Wilkins MR, Morrell NW. cAMP phosphodiesterase inhibitors potentiate effects of prostacyclin analogs in hypoxic pulmonary vascular remodeling. *Am J Physiol Lung Cell Mol Physiol* 2005;288:L103-L115.
30. Cortijo J, Iranzo A, Milara X, Mata M, Cerda-Nicolas M, Ruiz-Sauri A, Tenor H, Hatzelmann A, Morcillo EJ. Roflumilast, a phosphodiesterase 4 inhibitor, alleviates bleomycin-induced lung injury. *Br J Pharmacol* 2009;156:534-544.
31. Growcott EJ, Spink KG, Ren X, Afzal S, Banner KH, Wharton J. Phosphodiesterase type 4 expression and anti-proliferative effects in human pulmonary artery smooth muscle cells. *Respir Res* 2006;7:9.
32. De Franceschi L, Platt OS, Malpeli G, Janin A, Scarpa A, Leboeuf C, Beuzard Y, Payen E, Brugnara C. Protective effects of phosphodiesterase-4 (PDE-4) inhibition in the early phase of pulmonary arterial hypertension in transgenic sickle cell mice. *FASEB J* 2008;22:1849-1860.

33. Clapp LH, Finney P, Turcato S, Tran S, Rubin LJ, Tinker A. Differential effects of stable prostacyclin analogs on smooth muscle proliferation and cyclic AMP generation in human pulmonary artery. *Am J Respir Cell Mol Biol* 2002;26:194-201.
34. Schermuly RT, Yilmaz H, Ghofrani HA, Woyda K, Pullamsetti S, Schulz A, Gessler T, Dumitrescu R, Weissmann N, Grimminger F. Inhaled iloprost reverses vascular remodeling in chronic experimental pulmonary hypertension. *Am J Respir Crit Care Med* 2005;172:358-363.
35. Guignabert C, Raffestin B, Benferhat R, Raoul W, Zadigue P, Rideau D, Hamon M, Adnot S, Eddahibi S. Serotonin transporter inhibition prevents and reverses monocrotaline-induced pulmonary hypertension in rats. *Circulation* 2005;111:2812-2819.
36. Massaro D, Teich N, Maxwell S, Massaro GD, Whitney P. Postnatal development of alveoli. Regulation and evidence for a critical period in rats. *J Clin Invest* 1985;76:1297-1305.
37. Kasahara Y, Tudor RM, Taraseviciene-Stewart L, Le Cras TD, Abman S, Hirth PK, Waltenberger J, Voelkel NF. Inhibition of VEGF receptors causes lung cell apoptosis and emphysema. *J Clin Invest* 2000;106:1311-1319.
38. Thebaud B, Ladha F, Michelakis ED, Sawicka M, Thurston G, Eaton F, Hashimoto K, Harry G, Haromy A, Korbitt G. Vascular endothelial growth factor gene therapy increases survival, promotes lung angiogenesis, and prevents alveolar damage in hyperoxia-induced lung injury: evidence that angiogenesis participates in alveolarization. *Circulation* 2005;112:2477-2486.
39. Favot L, Keravis T, Holl V, Le Bec A, Lugnier C. VEGF-induced HUVEC migration and proliferation are decreased by PDE2 and PDE4 inhibitors. *Thromb Haemost* 2003;90:334-343.
40. D'Angelo G, Lee H, Weiner RI. cAMP-dependent protein kinase inhibits the mitogenic action of vascular endothelial growth factor and fibroblast growth factor in capillary endothelial cells by blocking Raf activation. *J Cell Biochem* 1997;67:353-366.
41. Netherton SJ, Maurice DH. Vascular endothelial cell cyclic nucleotide phosphodiesterases and regulated cell migration: implications in angiogenesis. *Mol Pharmacol* 2005;67:263-272.
42. Kunig AM, Balasubramaniam V, Markham NE, Morgan D, Montgomery G, Grover TR, Abman SH. Recombinant human VEGF treatment enhances alveolarization after hyperoxic lung injury in neonatal rats. *Am J Physiol Lung Cell Mol Physiol* 2005;289:L529-L535.
43. Kunig AM, Balasubramaniam V, Markham NE, Seedorf G, Gien J, Abman SH. Recombinant human VEGF treatment transiently increases lung edema but enhances lung structure after neonatal hyperoxia. *Am J Physiol Lung Cell Mol Physiol* 2006;291:L1068-L1078.
44. Donohue PK, Gilmore MM, Cristofalo E, Wilson RF, Weiner JZ, Lau BD, Robinson KA, Allen MC. Inhaled Nitric Oxide in Preterm Infants: A Systematic Review. *Pediatrics* 2011; 127(2):e414-22.

Appendice A

Online Data Supplement

Materials and Methods

Animals

Timed-pregnant Wistar rats were kept in a 12 h dark/light cycle and fed a standard chow diet (Special Diet Services, Witham, Essex, England) and drinking water ad libitum. Breeding pairs were allowed access for one hour on the day female rats showed very specific sexual behaviour: lordosis, hopping and air-flapping. After a gestation of approximately 21.5 days pregnant rats were killed by decapitation (spontaneous birth occurs 22 days after conception) and pups were delivered by hysterectomy through a median abdominal incision to ensure that the delay in birth between the first and the last pup is only 5 minutes. Immediately after birth, pups were dried and stimulated. Pups from four litters were pooled and distributed over four experimental groups: an oxygen (O₂) group, an oxygen-PDE4 inhibitor (O₂-piclamilast) group, a room air (RA) group, and a room air-PDE4 inhibitor (RA-piclamilast) group. Pups were kept in a transparent 50 x 50 x 70 cm plexiglas chamber during hyperoxia. In this way influences of the birth process within and between litters can be avoided and exposure to hyperoxia can be started within 30 min after birth. Pups were fed by lactating foster dams, which were rotated daily to avoid oxygen toxicity. All pups delivered by the foster dam were replaced by the experimental pups. Each foster dam nursed a litter of 12 pups in the experimental groups. Foster dams were exposed to 100% oxygen for 24 h and then to room air for 48 h. The oxygen concentration in the chamber was kept at 100% using a flow rate of 2.5 L/min. The oxygen concentration in the chamber was monitored daily with an oxygen sensor (Drägerwerk AG, Lübeck, Germany). Body weight, evidence of disease, and mortality were also checked daily. The research protocol was approved by the Institutional Animal Care and Use Committee of the Leiden University Medical Center.

Prophylactic treatment model

In this model neonatal lung injury was induced directly after birth (day 1) by continuous exposure to 100% oxygen for 3, 6 and 10 days (Figure E1A). Hyperoxia-exposed and room air-exposed pups were injected subcutaneously, starting on day 2, via a 0.5 mL syringe (U-100 Micro-Fine insulin 29G syringe, Becton Dickinson, Franklin Lakes, NJ, USA) at the lower back for 10 days. In the PDE4 inhibitor experiments pups received either 100 µL piclamilast (5.0 mg/kg/day; a gift from Nycomed GmbH, Konstanz, Germany) in 0.9% saline (containing 0.05-0.1% DMSO) or 100 µL 0.9% saline (containing 0.05-0.1% DMSO) in age-matched oxygen- and room air-exposed controls. Pups were sacrificed on day 1 (directly after hysterectomy), 3, 6 and 10. Separate experiments were performed for collection of lung and heart tissue for pulmonary fibrin deposition and RT-PCR (N=12), and histology (N=12).

Late treatment and injury-recovery model

The effects of piclamilast on lung injury and recovery were investigated by exposing newborn rat pups to hyperoxia for 9 days, followed by recovery in room air for 9 or 42 days (Figure

1B). After 6 days of exposure to hyperoxia, daily subcutaneous injections with either 100 μ L piclamilast (5.0 mg/kg/day) in 0.9% saline (containing 0.05-0.1% DMSO) or 100 μ L 0.9% saline (containing 0.05-0.1% DMSO) were started in age-matched oxygen- and room air-exposed controls and continued throughout a 9-day recovery period in room air. Lung and heart tissues were collected for histology at the end of the 9-day hyperoxia period (N=8), after the 9-day recovery period in room air (N=8) and after 6-weeks of recovery in room air (N=8).

Tissue preparation

Pups and adult rats were anesthetized with an intraperitoneal injection of ketamine (25 mg/kg body weight; Nimatek, Eurovet Animal Health BV, Bladel, The Netherlands) and xylazine (50 mg/kg body weight; Rompun, Bayer, Leverkusen, Germany). To avoid postmortem fibrin deposition in the lungs, heparin (100 units; Leo Pharma, Breda, The Netherlands) was injected intraperitoneally. After 5 min, pups were exsanguinated by transection of the abdominal blood vessels. The thoracic cavity was opened, and the lungs and heart were removed, snap-frozen in liquid nitrogen, and stored at -80°C until use for real-time RT-PCR or the fibrin deposition assay. For histology studies, the trachea was cannulated (Bioflow 0.6 mm intravenous catheter, Vygon, Veenendaal, the Netherlands) and the lungs were fixed in situ via the trachea cannula with buffered formaldehyde (4% paraformaldehyde in PBS, pH 7.4) at 27 cm H₂O pressure for 6 min. Lungs and heart were removed, fixed additionally in formaldehyde for 24 h at 4°C , and embedded in paraffin after dehydration in a graded alcohol series and xylene. To quantify the degree of right ventricular hypertrophy (RVH), hearts were harvested, followed by removal of the atria. Hereafter the right ventricular free wall (RV) was dissected, weighed separately from the interventricular septum (IVS) and left ventricle (LV), frozen immediately in liquid nitrogen, and stored at -80°C for RNA isolation. As an indicator of RVH the weight ratio $\text{RV}/(\text{LV} + \text{IVS})$ was calculated.

Histology

Lung paraffin sections (5 μ m) were cut and mounted onto SuperFrost plus-coated slides (Menzel, Braunschweig, Germany). After deparaffinization, lung sections were stained with hematoxylin and eosin (HE), with monoclonal anti- α -smooth muscle actin (ASMA) to visualize the pulmonary medial arterial walls, or with a rabbit polyclonal anti-von Willebrand Factor (vWF) antibody as a marker for pulmonary blood vessels¹. Heart sections were stained with HE or with a rabbit polyclonal anti-tenascin-C antibody. Extravascular tenascin-C expression was used as an indicator for cardiac tissue damage². For immunohistochemistry, sections were incubated with 0.3% H₂O₂ in methanol to block endogenous peroxidase activity. After a graded alcohol series, sections were boiled in 0.01 M sodium citrate (pH 6.0) for 10 min. Sections were incubated overnight with antibodies directed against ASMA (A2547, Sigma-Aldrich, St. Louis, MO, USA, diluted 1:10,000), vWF (A0082, Dako Cytomation, Glostrup, Denmark, diluted 1:4,000) or tenascin-C (SC-20932, Santa Cruz Biotechnology, Santa Cruz, CA, USA, diluted 1:500), stained with EnVision-HRP (Dako Cytomation, Glostrup, Denmark), using NovaRed (Vector, Burlingame, CA) as chromogenic substrate, and counterstained briefly with hematoxylin. Primary antibodies were diluted in 1% bovine serum albumin (fraction V, Roche Diagnostics, Almere, the Netherlands) in PBS.

For morphometry of the lung, an eye piece reticle with a coherent system of 21 lines and 42 points (Weibel type II ocular micrometer; Paes, Zoeterwoude, The Netherlands) was used. To investigate alveolar enlargement in experimental BPD we studied the number of alveolar crests to exclude potential effects of heterogenous alveolar development. The number of alveolar crests³ was assessed in 10 non-overlapping fields at a 400x magnification for each animal in ASMA-stained lung sections. Capillary density was determined in lung sections stained for vWF at a 200x magnification by counting the number of vessels per field. At least 10 representative fields per experimental animal were investigated. Results were expressed as relative number of vessels per mm². Pulmonary arteriolar wall thickness was measured in lung sections stained for ASMA at a 1000x magnification by averaging at least 10 vessels with a diameter of less than 30 μm per animal. Medial wall thickness was calculated from the formula⁴. Fields containing large blood vessels or bronchioli were excluded from the analysis. Thickness of the right and left ventricular free walls and interventricular septum (IVS) was assessed in a transversal HE-stained section taken halfway the long axis at a 40x magnification by averaging 6 measurements per structure. The number of right ventricles positive for extravascular tenascin-C staining was assessed by two independent investigators. For morphometric studies in lung and heart at least 10 rat pups per experimental group were studied. Quantitative morphometry was performed by two independent researchers blinded to the treatment strategy using the NIH Image J program.

Hemodynamic measurements

On day 18 (9 days recovery) RV pressure-volume loops were measured as previously described⁵. Briefly, rats were anesthetized with an intraperitoneal injection of ketamine (25 mg/kg body weight; Nimatek, Eurovet Animal Health BV, Bladel, the Netherlands) and xylazine (50 mg/kg body weight; Rompun, Bayer, Leverkusen, Germany). The rats were placed on a controlled warming pad to keep body temperature constant. A tracheotomy was performed, a 25-gauge cannula was inserted, and the animals were mechanically ventilated using a pressure-controlled respirator and a mixture of air and oxygen. The rats were placed under a stereomicroscope (Zeiss, Hamburg, Germany). After a midsternal thoracotomy was performed, a combined pressure-conductance catheter (model FT212, SciSense, London, Ontario, Canada) was introduced via the apex into the RV and positioned towards the pulmonary valve. The catheter was connected to a signal processor (FV898 Control Box, SciSense) and RV pressures and volumes were recorded digitally. All data were acquired at a sample rate of 2,000 Hz and analyzed off-line by custom-made software. After hemodynamic measurements, the heart was removed and fixed in buffered formaldehyde and processed for histology.

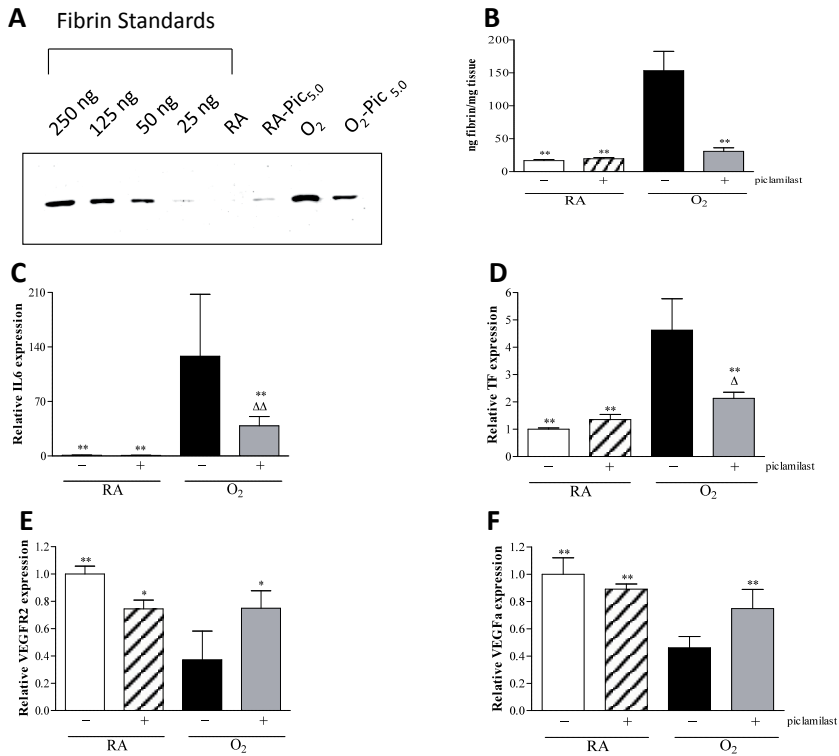
Fibrin detection assay

Fibrin deposition in lungs was detected as described previously⁶. Briefly, frozen lungs were homogenized with an Ultra-Turrax T25 basic tissue homogenizer (IKA-Werke, Staufen, Germany) for 1 min at full speed (24,000 rpm) in a cold 10 mM sodium phosphate buffer (pH 7.5), containing 5 mM EDTA, 100 mM β -aminocaproic acid, 10 U/ml aprotinin, 10 U/ml heparin, and 2 mM phenylmethanesulfonyl fluoride. The homogenate was incubated for 16 h on a roller bank at 4°C. After centrifugation (10,000 rpm, 4°C, 10 min), the pellet was resuspended in extraction buffer [10 mM sodium phosphate buffer (pH 7.5), 5 mM EDTA,

and 100 mM β -aminocaproic acid] and re-centrifuged. Pellets were suspended in 3 M urea, extracted for 2 h at 37°C, and centrifuged at 14,000 rpm for 15 min. After the supernatant was aspirated and discarded, the pellet was dissolved at 65°C in reducing sample buffer (10 mM Tris pH 7.5, 2% SDS, 5% glycerol, 5% β -mercaptoethanol, and 0.4 mg/ml bromophenol blue) for 90 min in a thermomixer (Eppendorf, Hamburg, Germany) with continuous mixing at 900 rpm. Hereafter, samples were subjected to SDS-PAGE (7.5%; 5% stacking) and blotted onto PVDF membrane (Immobilon-P, Millipore, Bredford, MA). The 56-kDa fibrin β -chains were detected with a monoclonal 59D8 antibody, followed by detection with an infrared labelled (IRDye 800CW; Licor Biosciences, Lincoln, NE, USA) goat-anti-mouse secondary antibody using an infrared detection system (Odyssey infrared imaging system, Licor Biosciences). Fibrin deposition was quantified in lungs of at least 10 rats per experimental group using rat fibrin as a reference ^{7;8}.

Real-time RT-PCR

Total RNA was isolated from lung and heart tissue homogenates using guanidium-phenol-chloroform extraction and isopropanol precipitation (RNA-Bee, Tel-Test Inc., Bio-Connect BV, Huissen, the Netherlands). The RNA sample was dissolved in RNase-free water and quantified spectrophotometrically. The integrity of the RNA was studied by gel electrophoresis on a 1% agarose gel, containing ethidium bromide. Samples did not show degradation of ribosomal RNA by visual inspection under ultraviolet light. First-strand cDNA synthesis was performed with the SuperScript Choice System (Life Technologies, Breda, the Netherlands) by mixing 2 μ g total RNA with 0.5 μ g of oligo(dT)12-18 primer in a total volume of 12 μ L. After the mixture was heated at 70°C for 10 min, a solution containing 50 mM Tris-HCl (pH 8.3), 75 mM KCl, 3 mM MgCl₂, 10 mM DTT, 0.5 mM dNTPs, 0.5 μ L RNase inhibitor, and 200 U Superscript Reverse Transcriptase was added, resulting in a total volume of 20.5 μ L. This mixture was incubated at 42°C for 1 h; total volume was adjusted to 100 μ L with RNase-free water and stored at -80°C until further use. For real-time quantitative PCR, 1 μ L of first-strand cDNA diluted 1:10 in RNase-free water was used in a total volume of 25 μ L, containing 12.5 μ L 2x SYBR Green PCR Master Mix (Applied Biosystems, Foster City, CA) and 200 ng of each primer. Primers, designed with the Primer Express software package (Applied Biosystems), are listed in Table E1. PCR reactions, consisting of 95°C for 10 min (1 cycle), 94°C for 15 s, and 60°C for 1 min (40 cycles), were performed on an ABI Prism 7900 HT Fast Real Time PCR system (Applied Biosystems) of the Leiden Genome Technology Center. Data were analyzed with the ABI Prism 7900 sequence detection system software (version 2.2.2) and quantified with the comparative threshold cycle method with β -actin as a housekeeping gene reference ⁹. In a DNA array experiment we demonstrated that β -actin was not differentially expressed in lungs of hyperoxic rat pups compared to room air controls ⁶. In addition β -actin was not differentially expressed in left and right ventricle in both control and experimental rat pups.

**Figure 1**

Western blot analysis of fibrin deposition in lung homogenates of rat pups exposed to room air (RA), RA in combination with 5.0 mg/kg/day of piclamilast (RA-Pic_{5.0}), oxygen (O₂) and O₂ in combination with 5.0 mg/kg/day of piclamilast (O₂-Pic_{5.0}) for 10 days (panel A). Panel B shows the quantification of fibrin deposition in lung homogenates on day 10. Relative mRNA expression in lungs, determined with RT-PCR, of genes related to inflammation (IL-6 [panel C]), coagulation (TF [panel D]) and alveolar growth (VEGFR2 [panel E] and VEGFa [panel F]). Experimental groups include room air controls (RA, white bar), room air-exposed rat pups treated with piclamilast (5.0 mg/kg/day; striped bar), age-matched oxygen-exposed controls (O₂, black bar) and oxygen-exposed rat pups treated with piclamilast (5.0 mg/kg/day; grey bar). Data are expressed as mean ± SEM (N=12). **p* < 0.05 and ***p* < 0.001 versus age-matched oxygen-exposed controls. ^Δ*p* < 0.01 and ^{ΔΔ}*p* < 0.001 versus room air-exposed controls treated with piclamilast.

Results

Effects of piclamilast on lung coagulation

Early concurrent treatment

Fibrin deposition was quantified (Figure E1B) after treatment with the PDE4 inhibitor piclamilast (5.0 mg/kg/day) in room air- and oxygen-exposed controls. Fibrin deposition was at background levels during normal neonatal pulmonary development without an effect of piclamilast treatment on day 10 (<25 ng fibrin/mg tissue in room air-exposed controls with

or without piclamilast). Fibrin deposition increased more than 9-fold to 153 ± 31 ng fibrin/mg tissue in lungs of pups exposed to 100% oxygen for 10 days ($p < 0.001$) compared to room air-exposed controls. Treatment with 5.0 mg/kg/day of piclamilast attenuated fibrin deposition 5-fold to 31 ± 5 ng fibrin/mg tissue compared to the oxygen-exposed controls ($p < 0.001$), which is a similar beneficial effect as described previously¹⁰.

mRNA expression in the lung

Early concurrent treatment

Treatment with piclamilast for 10 days during normal neonatal development did not result in differences in mRNA expression of IL6, TF, VEGFR2 and VEGFA compared to room air-exposed controls. Ten days of oxygen exposure resulted in an increase in mRNA expression of the pro-inflammatory cytokine IL-6 (128-fold; $p < 0.001$, Figure E1C) and the procoagulant factor tissue factor (TF, 4.6-fold; $p < 0.001$, Figure E1D), and a decrease in the expression of vascular endothelial growth factor receptor-2 (VEGFR2, 2.7-fold; $p < 0.001$, Figure E1E) and the growth factor VEGFA (2.2-fold; $p < 0.001$, Figure E1F) in lungs of oxygen-exposed compared to room air-exposed pups. Treatment with 5.0 mg/kg/day piclamilast in oxygen-exposed pups resulted in a reduction in IL-6 (by 69.8%; $p < 0.001$) and TF (by 53.9%; $p < 0.001$) mRNA expression compared to oxygen-exposed controls. In lung tissue of piclamilast-treated oxygen-exposed rat pups expression of VEGFR2 and VEGFA mRNA was increased by 101.6% ($p < 0.05$) and 62.2% ($p < 0.001$), respectively, compared to oxygen-exposed pups.

References

1. de Visser YP, Walther FJ, Laghmani EH, van der Laarse A, Wagenaar GT. Apelin attenuates hyperoxic lung and heart injury in neonatal rats. *Am J Respir Crit Care Med* 2010;182: 1239-1250.
2. Hessel MHM, Steendijk P, den Adel B, Schutte CI, van der Laarse A. Pressure Overload-Induced Right Ventricular Dilatation is Associated with Re-Expression of Myocardial Tenascin-C and Increased Plasma Levels of Tenascin-C. *Circulation* 2006;114:II: 133.
3. Yi M, Jankov RP, Belcastro R, Humes D, Copland I, Shek S, Sweezey NB, Post M, Albertine KH, Auten RL, Tanswell AK. Opposing effects of 60% oxygen and neutrophil influx on alveologenesis in the neonatal rat. *Am J Respir Crit Care Med* 2004;170: 1188-1196.
4. Koppel R, Han RN, Cox D, Tanswell AK, Rabinovitch M. Alpha 1-antitrypsin protects neonatal rats from pulmonary vascular and parenchymal effects of oxygen toxicity. *Pediatr Res* 1994;36: 763-770.
5. Hessel MH, Steendijk P, den Adel B, Schutte CI, van der Laarse A. Characterization of right ventricular function after monocrotaline-induced pulmonary hypertension in the intact rat. *Am J Physiol Heart Circ Physiol* 2006;291: H2424-H2430.
6. Wagenaar GT, ter Horst SA, van Gastelen MA, Leijser LM, Mauad T, van der Velden PA, de Heer E, Hiemstra PS, Poorthuis BJ, Walther FJ. Gene expression profile and histopathology of experimental bronchopulmonary dysplasia induced by prolonged oxidative stress. *Free Radic Biol Med* 2004;36: 782-801.
7. Dijkstra CD, Dopp EA, Joling P, Kraal G. The heterogeneity of mononuclear phagocytes in lymphoid organs: distinct macrophage subpopulations in the rat recognized by monoclonal antibodies ED1, ED2 and ED3. *Immunology* 1985;54: 589-599.
8. Hui KY, Haber E, Matsueda GR. Monoclonal antibodies to a synthetic fibrin-like peptide bind to human fibrin but not fibrinogen. *Science* 1983;22: 1129-1132.
9. Pfaffl MW. A new mathematical model for relative quantification in real-time RT-PCR. *Nucleic Acids Res* 2001;29: e45.
10. de Visser YP, Walther FJ, Laghmani EH, van Wijngaarden S, Nieuwland K, Wagenaar GT. Phosphodiesterase 4 inhibition attenuates pulmonary inflammation in neonatal lung injury. *Eur Respir J* 2008;31: 633-644.

